


Article

# Dosimetric Issues Associated with Percutaneous Ablation of Small Liver Lesions with $^{90}\text{Y}$

Marco D'Arienzo <sup>1,2,†</sup>, Anna Sarnelli <sup>3,\*</sup>,†, Emilio Mezzenga <sup>3</sup> , Laura Chiacchiararelli <sup>4</sup>,  
Antonino Amato <sup>5</sup>, Massimo Romanelli <sup>5</sup>, Roberto Cianni <sup>6</sup>, Marta Cremonesi <sup>7</sup>  
and Giovanni Paganelli <sup>8</sup>

<sup>1</sup> ENEA, Italian National Institute of Ionizing Radiation Metrology, Via Anguillarese 301, 00123 Rome, Italy; marco.darienzo@enea.it

<sup>2</sup> ASL Roma 6, Medical Physics Unit, Borgo Garibaldi, 12, 00041 Albano Laziale, Italy

<sup>3</sup> Medical Physics Unit, Istituto Scientifico Romagnolo per lo Studio e la Cura dei Tumori (IRST) IRCCS, Via Piero Maroncelli 40, 47014 Meldola, Italy; emilio.mezzenga@irst.emr.it

<sup>4</sup> Medical Physics Unit, Ospedale Sant'Andrea, Via di Grottarossa 1035, 00189 Rome, Italy; laurac@ospedalesantandrea.it

<sup>5</sup> BetaGlue Technologies Spa, Lungadige Galtarossa 21, 37133 Verona, Italy; a.amato@betaglu.com (A.A.); m.romanelli@betaglu.com (M.R.)

<sup>6</sup> Radiology Unit, San Camillo-Forlanini hospital, Circonvallazione Gianicolense 87, 00152 Rome, Italy; rcianni@scamilloforlanini.rm.it

<sup>7</sup> Medical Physics Unit, European Institute of Oncology, Via Ripamonti 435, I-20132 Milano, Italy; marta.cremonesi@ieo.it

<sup>8</sup> Nuclear Medicine Unit, Istituto Scientifico Romagnolo per lo Studio e la Cura dei Tumori (IRST) IRCCS, Via Piero Maroncelli 40, 47014 Meldola, Italy; giovanni.paganelli@irst.emr.it

\* Correspondence: anna.sarnelli@irst.emr.it

† These authors contributed equally to this work.

Received: 21 August 2020; Accepted: 16 September 2020; Published: 22 September 2020



**Abstract:** The aim of the present paper is twofold. Firstly, to assess the absorbed dose in small lesions using Monte Carlo calculations in a scenario of intratumoral injection of  $^{90}\text{Y}$  (e.g., percutaneous ablation). Secondly, to derive a practical analytical formula for the calculation of the absorbed dose that incorporates the absorbed fractions for  $^{90}\text{Y}$ . The absorbed dose per unit administered activity was assessed using Monte Carlo calculations in spheres of different size (diameter 0.5–20 cm). The spheres are representative of tumor regions and are assumed to be uniformly filled with  $^{90}\text{Y}$ . Monte Carlo results were compared with the macrodosimetric approach used for dose calculation in liver radioembolization. The results of this analysis indicate that the use of the analytic model provides dose overestimates below 10% for lesions with diameter larger than approximately 2 cm. However, for lesions smaller than 2 cm the analytic model is likely to deviate significantly (>10%) from Monte Carlo results, providing dose overestimations larger than 50% for lesions of 0.5 cm diameter. In this paper an analytical formula derived from MC calculations that incorporates the absorbed fractions for  $^{90}\text{Y}$  is proposed. In a scenario of intratumoral injection of microspheres, the proposed equation can be usefully employed in the treatment planning of spherical lesions of small size (down to 0.5 cm diameter) providing dose estimates in close agreement with Monte Carlo calculations (maximum deviation below 0.5%).

**Keywords:** percutaneous radioablation; monte carlo dosimetry; liver lesions; molecular radiotherapy

## 1. Introduction

Hepatocellular carcinoma (HCC) is the most common primary liver malignancy and today multiple treatment modalities exist [1]. Due to the lack of effective systemic therapies for HCC, researchers have been investigating the use of locoregional tumor control with  $^{90}\text{Y}$  radioembolization since the 1960s. Today radioembolization (or Selective Internal Radio Therapy, SIRT) is an established and effective treatment for liver malignancies based on trans-arterial infusion of  $^{90}\text{Y}$ -laden microspheres [2–4]. At present, there are two clinically available microsphere devices in which  $^{90}\text{Y}$  is incorporated: one with microspheres made of glass (TheraSphere; MDS Nordion, Ottawa, ON, Canada) and the other with microspheres made of resin (SIR-Spheres; Sirtex Medical, Sydney, Australia). Once administered, the spheres remain in the liver as a permanent implant.

Radiation dose distributions arising from intrahepatic arterial infusion of  $^{90}\text{Y}$  microspheres have been investigated by a number of authors in the past. In recent years a number of studies have addressed the problem of dosimetry in therapies based on the use of intratumoral administration of  $^{90}\text{Y}$ -conjugates by percutaneous puncture. This technique has been successfully applied to patients treated with  $^{90}\text{Y}$ -labeled [DOTA<sup>0</sup>-D-Phe<sup>1</sup>-Tyr<sup>3</sup>]octreotide ( $^{90}\text{Y}$ -DOTATOC) for malignant gliomas [5–7]. In fact, based on the clinical experience gained in liver radioembolization, it is reasonable to assume that percutaneous ablation of HCC through the intratumoral injection of an appropriate activity of  $^{90}\text{Y}$  has the potential to reduce drastically the chances of local recurrence. In this context, there is growing interest in the development of new intratumoral procedures for HCC throughout a localized administration of  $^{90}\text{Y}$  in the form of microspheres mixed with biocompatible compounds [8].

As a general rule, intratumoral administration of radionuclides raises questions about the dosimetry of small lesions as this approach allows sub-centimeters tumors to be selectively treated [9,10]. To date, there is no simple way to assess exactly the absorbed dose to tumours and normal liver when  $^{90}\text{Y}$  is administered. This is because  $^{90}\text{Y}$  only emits pure beta radiation with limited penetration range in tissue. As a consequence, the delivered dose is highly dependent on the distribution of the radionuclide and the tumor mass.

Calculation of the radiation dose to tumors may require consideration of the losses of electron energy. In the traditional macrodosimetric approach, all of the electron energy emitted in a source region is assumed to be absorbed in that region. This is quite reasonable for most situations because the range of most electrons in body tissues is small compared to the size of most source regions. However, when the tumor size is small this assumption is no longer true and the absorbed fraction may be significantly less than unity. Some preliminary work dedicated to the assessment of the absorbed fractions for beta particles in spherical regions of different sizes was carried out in the early 1990s by Siegel [11] and Bardies [12]. In a major advance in 2000 Stabin and Konijnenberg [13] reevaluated and updated absorbed fractions in spherical regions comparing different Monte Carlo codes, while in 2010 Amato and colleagues [14] calculated absorbed fractions for electrons in ellipsoidal volumes. The aim of the present paper is to assess the absorbed dose of  $^{90}\text{Y}$  after percutaneous administration in small spherical lesions proposing a practical analytical formula that incorporates the absorbed fractions for  $^{90}\text{Y}$ . Of note, in [13] absorbed fractions were assessed for monoenergetic electrons using MCNP version 4B, while in this study absorbed dose fractions were calculated implementing the full  $^{90}\text{Y}$  spectrum and using an upgraded version of MCNP (version 4C). Calculations were performed assuming both water and liver density ( $\rho = 1.00 \text{ g/cm}^3$  and  $\rho = 1.05 \text{ g/cm}^3$ , respectively) for spheres of different diameter (0.5–20 cm). MC results were then compared with the well established macrodosimetric approach used for the dose assessment in liver radioembolization Equation (4).

## 2. Materials and Methods

### 2.1. Percutaneous Ablation with $^{90}\text{Y}$

Recently, it has been proposed the intralesional injection of  $^{90}\text{Y}$  in the form of resin microspheres embedded in a bio-compatible matrix. The injection is performed using a proprietary delivery

system [8]. This procedure is also known as percutaneous radioablation and is a minimally invasive treatment for patients with small (below approximately 3 to 5 cm) liver tumors performed using BAT-90, a combination of the following components: (i) BioGlue® (Cryolife, Atlanta, GA, USA), a FDA-approved mixture of bovine serum albumin (45%) and glutaraldehyde (10%) in a 4:1 ratio, approved for use in soft tissue repair or to seal damaged parenchyma [15] (ii) SIR-Spheres® coated with <sup>90</sup>Y (Sirtex Medical, Sydney, Australia) approved for implantation into hepatic tumors via the hepatic artery. BAT-90 is percutaneously injected through the MIPP-Kit® (Svas Biosana, Naples, Italy) a dedicated coaxial dual-lumen catheter for the direct, imaging-guided intra-tumoral injection.

The two components of BAT-90 are dispensed from a double-barrel syringe and mix within the delivery tip in a predefined ratio. The adhesive begins to polymerize within 20–30 s and reaches maximum bonding strength in 2 min. Once injected into the tumor region, the radiopharmaceutical combination (BAT-90) remains in the lesion delivering the required tumoricidal dose. As a consequence, in order to simulate a scenario of percutaneous ablation, in the present study we assumed that <sup>90</sup>Y is homogeneously dispersed into the lesion and that there is no biological removal of the radiopharmaceutical.

## 2.2. Dosimetry with <sup>90</sup>Y

<sup>90</sup>Y disintegrates by  $\beta$  emission mainly (99.983% [16]) to the stable <sup>90</sup>Y ground state level. A weak beta branch occurs to the 1760 keV excited level which decays by a E0 gamma transition [16]. This 0<sup>+</sup>-0<sup>+</sup> transition is followed by the emission of two gammas, or an electron-positron pair, or internal conversion. The adopted half life of <sup>90</sup>Y ground state is 64.041(31) h or 2.6684(13) days [16].

Among the radionuclides used in clinical practice, <sup>90</sup>Y has attractive physical and radiobiologic features that make this radionuclide suitable for a loco-regional therapeutic option. The high-energy  $\beta$ -particles (maximum energy 2278.7(16) keV, average energy 926.7(8) keV [16]) and their penetration depth (maximum particle range in tissue, 11 mm; range in tissue after which 50% of the energy particles is transferred, 4 mm) allows high radiation doses to be selectively delivered to the target area, while sparing surrounding tissues and normal organs. In particular, the penetration depth of the high-energy  $\beta$ -particles is a key element of this radionuclide's success in radioembolization, allowing for high-dose deposition into the tissues between embolized capillars. In the traditional dose calculation formalism (after locoregional administration of <sup>90</sup>Y) two important simplifying assumptions are generally made:

- $\beta$  radiation released from <sup>90</sup>Y within a given organ is fully absorbed by that organ. In most cases, this assumption is supported by the average 4 mm <sup>90</sup>Y  $\beta$  range in tissue.
- permanence of <sup>90</sup>Y in the area where they have been delivered (i.e., no migration of the radiopharmaceutical outside the tumor region).

Combining these two assumptions allows for easy calculation of average absorbed dose to an organ of interest on a macroscopic scale. The calculation, carried out using most up-to-date nuclear data for <sup>90</sup>Y [16], is illustrated below and it is generally referred to as the MIRD approach [17]:

$$E_{avg} = \int_0^{\infty} E\varphi(E)dE = 926.7 \text{ keV} = 1.4847 \times 10^{-13} \text{ J} \quad (1)$$

$$E_{tot} = A_0 E_{avg} \int_0^{\infty} e^{-\lambda t} dt = \frac{A_0}{\lambda} (1.4847 \times 10^{-13} \text{ J}) = A_0 \cdot k \quad (2)$$

where  $E_{avg}$  is the average energy released per decay of <sup>90</sup>Y based on the probability density function  $\varphi(E)$  for emission,  $\lambda$  is the <sup>90</sup>Y decay constant based on the half-life of 64.041(31) hours, and  $k$  a constant term.  $A_0$  is the activity present in the organ in GBq and  $E_{tot}$  is the total energy released by  $A_0$  from the time that it is infused until it has fully decayed.

Assuming that all of the energy of the  $\beta^-$  decay is absorbed in the volume where the decay occurs, the constant term,  $k$ , can be calculated taking the given physical values and their statistical uncertainties:

$$k = \frac{1.4847 \times 10^{-13} \text{ J}}{\lambda} = \frac{1.4847 \times 10^{-13} \text{ J} \times 230547 \text{ s}}{0.69315} \times \frac{10^9 \text{ dis/s}}{\text{GBq}} = 49.38(5) \text{ (J/GBq)} \quad (3)$$

The constant factor 49.38 (J/GBq) is the energy released per unit activity of  $^{90}\text{Y}$ . The adopted uncertainties on the nuclear data [16] reported in Equation (4) lead to a relative standard uncertainty of 0.1% on the constant term, i.e., 49.38(5) (J/GBq), in line with [18].

Finally, the absorbed dose  $D$  (expressed in Gy) can be obtained by dividing the delivered energy,  $E_{tot}$ , by the mass of the target region  $m$  (expressed in kg):

$$D_{avg} \text{ (Gy)} = \frac{A_0 \text{ (GBq)} \times 49.38(5) \text{ (J/GBq)}}{m \text{ (kg)}} \quad (4)$$

Of note, the same formula with a slightly different constant term,  $k$ , is reported in other publications (e.g., 49.98 [17], 49.67 [19]).

According to the partition model [20–22], Equation (4) can be used to calculate the absorbed dose in the tumor, once the fractional tumor uptake  $FU_{tumor}$  (i.e., the fraction of the administered activity accumulated in the tumor) is known:

$$D_{tumor} \text{ (Gy)} = \frac{A_0 \text{ (GBq)} \times 49.38(5) \text{ (J/GBq)} \times FU_{tumor}}{m \text{ (kg)}} \quad (5)$$

It must be reiterated that Equations (4) and (5) are representative of average absorbed dose on a macroscopic scale, i.e., on an organ or a large lesion where the absorbed fraction can be assumed equal to unity. These equations may not hold for very small tumor masses, as the assumption that the energy emitted during decay is totally absorbed by the mass of interest  $m$  is no longer true. In particular, when the size of the lesion is very small (especially in the sub-centimeter region), the energy released per unit activity of  $^{90}\text{Y}$  may decrease significantly. As a consequence hereafter the constant term  $k$  in Equation (3) will be treated as a function of the lesion radius ( $r$ ) and indicated as  $k(r)$ .

### Monte Carlo Calculations

In the present study the absorbed dose per unit administered activity was assessed using Monte Carlo calculations in a simplified geometry. MC code MCNP4C has been used for this purpose [23]. MCNP is a general-purpose, continuous-energy, generalized-geometry, time-dependent, coupled neutron/photon/electron Monte Carlo transport code. For photon transport, the code takes into account photoelectric absorption, with the possibility of K- and L-shell fluorescent emission or Auger electron, coherent and incoherent scattering and pair production. The photoelectric cross sections are based on Storm and Israel [24] whereas the scattering cross sections are taken from ENDF tabulations [25]. The continuous slowing down approximation energy loss model is used for electron transport.

Spherical lesions of different size (diameter in the range 0.5–20 cm) were simulated for two different densities:  $\rho = 1.00 \text{ g/cm}^3$  (water density) and  $\rho = 1.05 \text{ g/cm}^3$  (liver density). In both scenarios, spheres were assumed to be immersed in a semi-infinite medium with the same density of the sphere. The spheres are representative of tumor regions and are supposed to be uniformly filled with  $^{90}\text{Y}$ , while the surrounding medium is assumed to contain no radioactivity.

Calculations were performed in coupled electron-photon mode [MODE P E] using the el03 electron interaction data library (ELIB = 03E) and the mcnp1ip2 photon interaction data library (PLIB = 02P). Simulations were carried out taking into account all the available advanced options such as electron

production by photons, Bremsstrahlung effect and knock-on electron production. MCNP simulations were run for an adequate time to get a statistical uncertainty on the absorbed dose below 0.01%.

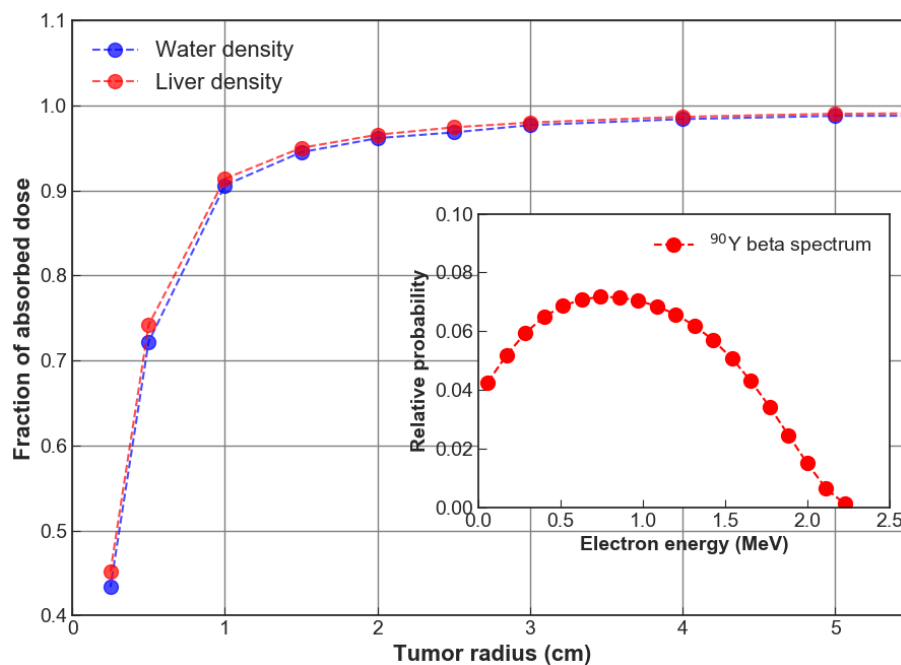
### 3. Results

Figure 1 shows the fraction of  $^{90}\text{Y}$  absorbed dose into the tumor as a function of the tumor size, obtained from MCNP simulations. The  $^{90}\text{Y}$  beta spectrum implemented in the model is also reported in the same figure. Calculations were performed both for water spheres ( $\rho = 1.00 \text{ g/cm}^3$ ) and for spheres made of liver tissue ( $\rho = 1.05 \text{ g/cm}^3$ ). In both cases, when the lesion diameter drops below 2 cm, a great amount of the  $\beta$  particle energy is delivered outside the sphere. Consistently, the delivered energy per unit activity,  $k(r)$ , shows the same trend (Figure 2) confirming that when the tumor size is small such term deviates significantly from the value  $49.38 \text{ (J/GBq)}$ , considered in Equation (4). In order to use information reported in Figure 2 at the clinical level,  $k(r)$  data obtained from MC calculations were fitted with the following function:

$$k(r) = k_0 + A \cdot (1 - \exp(-\frac{r}{a})) + B \cdot (1 - \exp(-\frac{r}{b})) \tag{6}$$

where  $r$  is the lesion radius in  $\text{cm}$  (assuming spherical tumors) and  $k_0, A, a, B, b$  are parameters determined by the fit (reported in Table 1 both for water and liver density). An  $r^2 = 0.999$  was obtained from the fit, both for water and liver density. Furthermore, goodness-of-fit was also assessed through the analysis of residuals (Figure 2B), which shows maximum deviations below 0.2 between calculated and fitted data, confirming the accuracy of the fit. Based on the fitting function described in Equation (6), Equation (4) can be rewritten in the following form:

$$D_{avg}(r) = \frac{A_0 \cdot k(r)}{m} \tag{7}$$



**Figure 1.** Fraction of  $^{90}\text{Y}$  absorbed dose into the tumor as a function of the tumor size. Simulations were performed for  $\rho = 1.00 \text{ g/cm}^3$  (water density) and  $\rho = 1.05 \text{ g/cm}^3$  (liver density). Inset:  $^{90}\text{Y}$  beta spectrum implemented in the model.

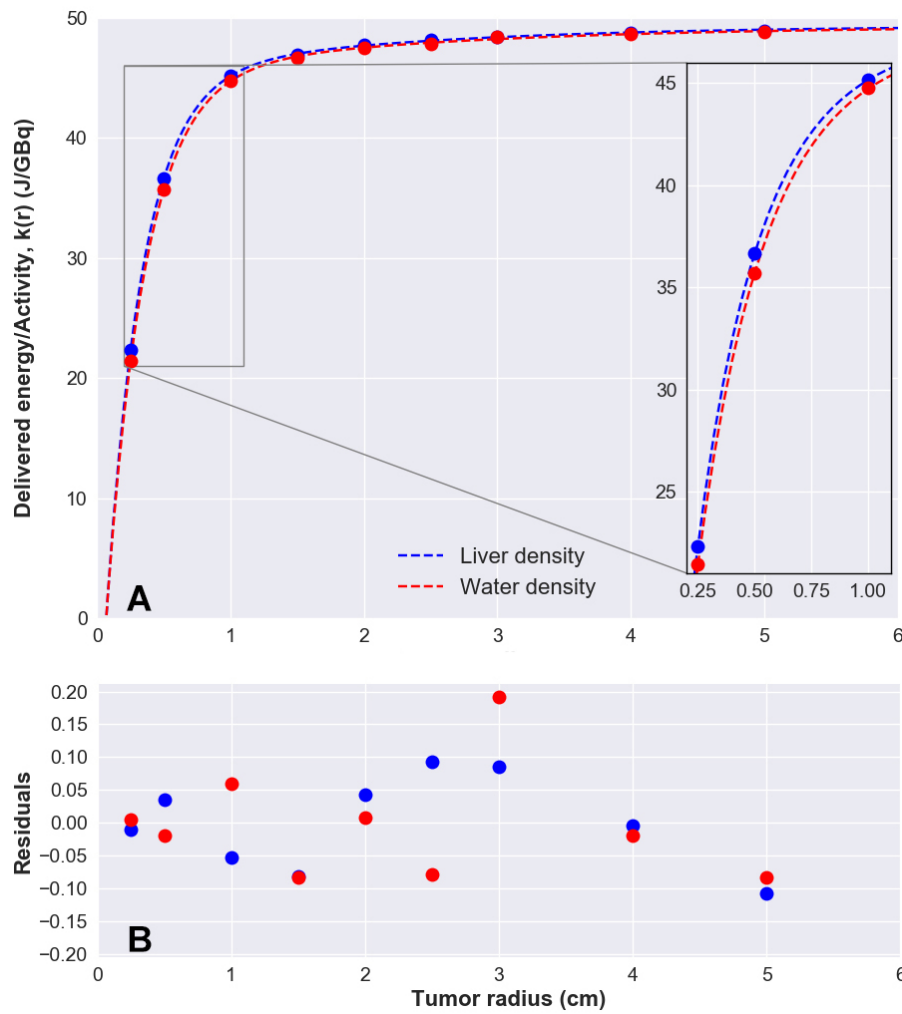


**Figure 2.** (A) Delivered energy per unit activity of  $^{90}\text{Y}$ ,  $k(r)$ , calculated with MCNP4c as a function of the tumor diameter. Data were fitted with Equation (6). (B) Analysis of residuals.

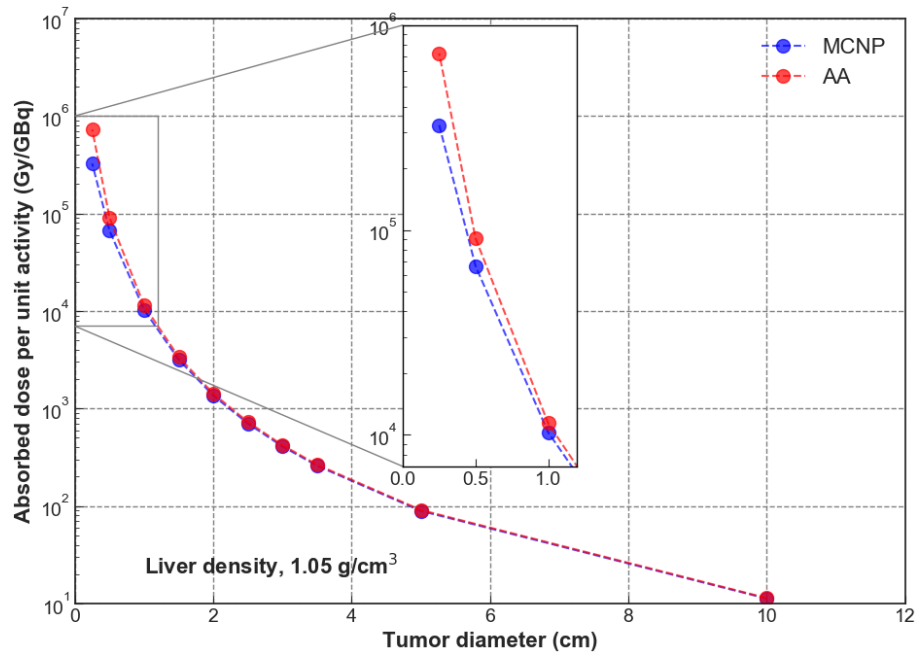
**Table 1.** Fitting parameters of Equation (6) with relative standard uncertainties, for water and liver density (denoted with superscripts  $^W$  and  $^L$ , respectively).  $R^2 = 0.999$  in both cases.

Parameter	Value <sup>W</sup>	$u_{\text{rel}}^{\text{W}/\%}$	Value <sup>L</sup>	$u_{\text{rel}}^{\text{L}/\%}$
$k_0$	-11.883	1.10	-12.999	1.00
A	4.416	1.15	4.654	1.10
a	2.190	0.90	1.909	1.00
B	56.820	0.05	57.701	0.05
b	0.290	0.15	0.271	0.10

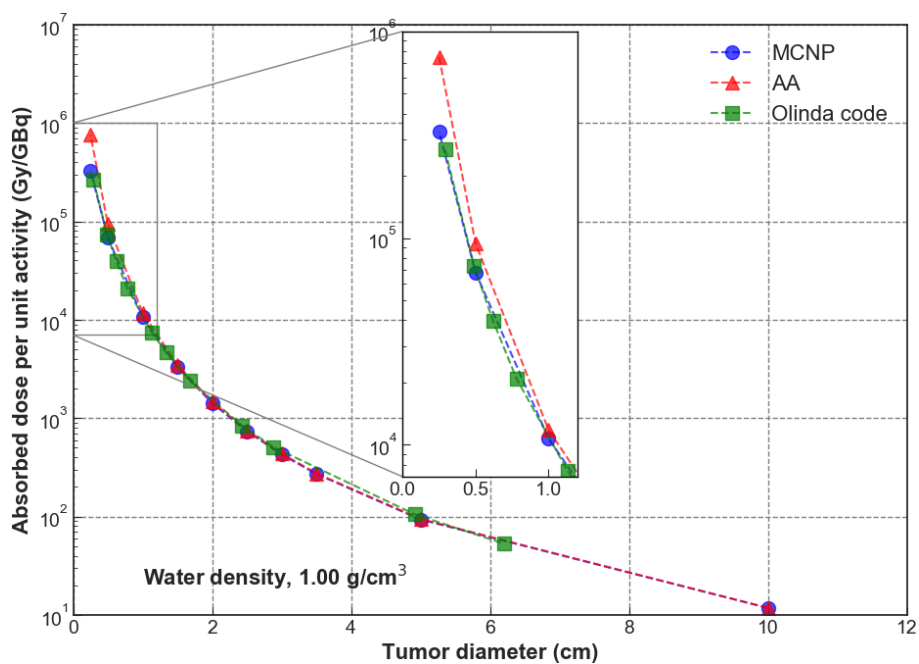
For a given activity  $A_0$ , Equation (7) can be used to accurately calculate the absorbed dose for very small lesions (down to 0.5 cm diameter). The absorbed dose to lesions calculated using Equation (7) provides results in good agreement with MC calculations (maximum deviation below 0.5%). As expected, when ideally  $r \rightarrow \infty$  Equation (7) reduces to Equation (4). Of note, the energy per unit activity,  $k(r)$ , obtained from Equation (6) when  $x \rightarrow \infty$  is 49.35 (J/GBq), against the accepted value of 49.38 (J/GBq) derived from Equation (4) (0.06% deviation).

Figure 3 compares absorbed doses per unit activity (Gy/GBq) calculated with Monte Carlo with those obtained using the analytic approach described by Equation (4), for spherical lesions of different size and for  $\rho = 1.05 \text{ g/cm}^3$ . The same results for  $\rho = 1.00 \text{ g/cm}^3$  are shown in Figure 4.

In addition Figure 4 reports absorbed doses calculated using the well established Olinda/EXM code, developed by the RADiation Dose Assessment Resource (RADAR) Task Group of the Society of Nuclear Medicine [26]. As illustrated in Figure 4, absorbed dose values calculated with MC approach concur well with those obtained using Olinda/EMX. Significant deviations were found between MC calculated dose values and those obtained using the analytic formulation when the lesion diameter drops below 2 cm (Figure 4, inset).



**Figure 3.** Absorbed dose per unit administered activity (GBq), for  $\rho = 1.05 \text{ g/cm}^3$  (liver density). Comparison between MC approach (MCNP) and the analytical formulation (AA) described by Equation (4). Inset: detail in the range 0 cm–1 cm lesion size.



**Figure 4.** Absorbed dose per unit administered activity (GBq), for  $\rho = 1.00 \text{ g/cm}^3$  (water density). Comparison between MC approach (MCNP) and the analytical formulation (AA) described by Equation (4). Inset: detail in the range 0 cm–1 cm lesion size.

Ultimately, Tables 2 and 3 compare absorbed dose values per GBq of administered activity obtained with MC calculations ( $D_{MCNP}$ ) and with the analytical approach reported in Equation (4), ( $D_{AA}$ ). The percentage differences between the two methods (last column of both tables,  $\Delta$ ) is also reported, calculated as  $100 \cdot (D_{MCNP} - D_{AA})/D_{AA}$ . The difference in absorbed dose values is within  $\sim 10\%$  as long as the diameter of the lesion exceeds 2 cm. The two calculation approaches deviate significantly when the lesion size drops below 2 cm, due to significant energy deposition outside the sphere. This is consistent with the maximum particle range in tissue for  $^{90}\text{Y}$  (about 11 mm). In this case, for water (liver) density MC calculations provide absorbed doses  $-9.3\%$  ( $-9.6\%$ ),  $-27.8\%$  ( $-26.7\%$ ),  $-56.7\%$  ( $-55.4\%$ ) lower than those obtained using the analytic formulation described by Equation (4) for tumor diameter of 2 cm, 1 cm and 0.5 cm, respectively (Tables 2 and 3).

**Table 2.** Dose per unit activity calculated with MCNP4C for spherical lesions of different size uniformly filled with  $^{90}\text{Y}$ . The lesions are assumed to have a density of  $\rho = 1.05 \text{ g/cm}^3$  (liver density). The same quantity (dose per unit activity) has been calculated using the analytic approach (AA) described by Equation (4). The last column of the table ( $\Delta$ ) shows the percentage deviation between the two methods, calculated as  $100 \cdot (D_{MCNP} - D_{AA})/D_{AA}$ .

Lesion Diameter	Mass (kg)	Dose/Particle (Gy/p)	MCNP (Gy/GBq)	AA (Gy/GBq)	$\Delta$
20 cm	4.40	$3.38 \times 10^{-14}$	$1.12 \times 10^1$	$1.14 \times 10^1$	$-1.8\%$
10 cm	$5.50 \times 10^{-1}$	$2.68 \times 10^{-13}$	$8.91 \times 10^1$	$9.10 \times 10^1$	$-2.1\%$
8.0 cm	$2.81 \times 10^{-1}$	$5.21 \times 10^{-13}$	$1.73 \times 10^2$	$1.78 \times 10^2$	$-2.5\%$
6.0 cm	$1.19 \times 10^{-1}$	$1.23 \times 10^{-12}$	$4.08 \times 10^2$	$4.21 \times 10^2$	$-3.1\%$
5.0 cm	$6.87 \times 10^{-2}$	$2.11 \times 10^{-12}$	$7.01 \times 10^2$	$7.28 \times 10^2$	$-3.7\%$
4.0 cm	$3.52 \times 10^{-2}$	$4.08 \times 10^{-12}$	$1.36 \times 10^3$	$1.42 \times 10^3$	$-4.2\%$
3.0 cm	$1.48 \times 10^{-3}$	$9.51 \times 10^{-12}$	$3.16 \times 10^3$	$3.34 \times 10^3$	$-6.2\%$
2.0 cm	$4.40 \times 10^{-3}$	$3.09 \times 10^{-11}$	$1.03 \times 10^4$	$1.14 \times 10^4$	$-9.6\%$
1.0 cm	$5.50 \times 10^{-4}$	$2.01 \times 10^{-10}$	$6.67 \times 10^4$	$9.10 \times 10^4$	$-26.7\%$
0.5 cm	$6.87 \times 10^{-5}$	$9.77 \times 10^{-10}$	$3.25 \times 10^5$	$7.28 \times 10^5$	$-55.4\%$

**Table 3.** Dose per unit activity calculated with MCNP for spherical lesions of different size uniformly filled with  $^{90}\text{Y}$ . The lesions are assumed to have a density of  $\rho = 1 \text{ g/cm}^3$  (water density). The same quantity (dose per unit activity) has been calculated using the analytic approach (AA) described by Equation (4). The last column of the table ( $\Delta$ ) shows the percentage deviation between the two methods, calculated as  $100 \cdot (D_{MCNP} - D_{AA})/D_{AA}$ .

Lesion Diameter	Mass (kg)	Dose/Particle (Gy/p)	MCNP (Gy/GBq)	AA (Gy/GBq)	$\Delta$
20 cm	4.19	$3.54 \times 10^{-14}$	$1.18 \times 10^1$	$1.18 \times 10^1$	0.0%
10 cm	$5.23 \times 10^{-1}$	$2.81 \times 10^{-13}$	$9.33 \times 10^1$	$9.44 \times 10^1$	$-1.2\%$
8.0 cm	$2.68 \times 10^{-1}$	$5.47 \times 10^{-13}$	$1.81 \times 10^2$	$1.84 \times 10^2$	$-1.5\%$
6.0 cm	$1.13 \times 10^{-1}$	$1.29 \times 10^{-12}$	$4.27 \times 10^2$	$4.37 \times 10^2$	$-2.3\%$
5.0 cm	$6.54 \times 10^{-2}$	$2.20 \times 10^{-12}$	$7.31 \times 10^2$	$7.55 \times 10^2$	$-3.2\%$
4.0 cm	$3.35 \times 10^{-2}$	$4.27 \times 10^{-12}$	$1.42 \times 10^3$	$1.47 \times 10^3$	$-3.4\%$
3.0 cm	$1.41 \times 10^{-3}$	$9.95 \times 10^{-12}$	$3.30 \times 10^3$	$3.49 \times 10^3$	$-5.4\%$
2.0 cm	$4.19 \times 10^{-3}$	$3.22 \times 10^{-11}$	$1.07 \times 10^4$	$1.18 \times 10^4$	$-9.3\%$
1.0 cm	$5.23 \times 10^{-4}$	$2.05 \times 10^{-10}$	$6.82 \times 10^4$	$9.44 \times 10^4$	$-27.8\%$
0.5 cm	$6.54 \times 10^{-5}$	$9.86 \times 10^{-10}$	$3.27 \times 10^5$	$7.55 \times 10^5$	$-56.7\%$



#### 4. Discussion

Molecular radiotherapy with  $^{90}\text{Y}$  has received much attention in the past two decades and the dosimetry of small lesions remains a key issue. The maximum range of  $^{90}\text{Y}$   $\beta$ -particles is 11 mm in tissue, while its average energy  $\beta$ -particles has a range of about 2.5 mm. It is worth noting that the penetration depth of the high-energy  $^{90}\text{Y}$   $\beta$ -particles is a critical component of this radionuclide's success in liver radioembolization, allowing for high dose delivery into the tissue between embolized capillars. Previous work has been dedicated to the assessment of absorbed fractions for electrons and beta particles in spheres [11–13] and ellipsoidal volumes [14] of various sizes. The present study focused on the assessment of the absorbed dose per unit activity in a scenario of percutaneous ablation of HCC through the intratumoral injection of  $^{90}\text{Y}$  in lesions of varying size. A simplified model tumor areas was implemented into MCNP4C MC code with the aim to determine the absorbed dose to the lesion when the tumor mass is uniformly filled with  $^{90}\text{Y}$ . Spherical lesions of different size (diameter in the range 0.5–20 cm) were simulated for two different densities:  $\rho = 1.00 \text{ g/cm}^3$  (water density) and  $\rho = 1.05 \text{ g/cm}^3$  (liver density). In both scenarios, lesions were assumed to be immersed in a semi-infinite medium with the same density of the lesion.

The problem of beta dosimetry in small lesions is not new [11–13]. Absorbed fractions calculated in this study are hardly comparable with those assessed in [11,13] as the authors performed calculations assuming monoenergetic electrons, while in this study the full  $^{90}\text{Y}$  spectrum was implemented. Furthermore, in [13] the authors used MCNP4B, while in this work MCNP4C was used instead.

The widely used analytic approach described by Equation (4) and MCNP calculations provide results in close agreement (within 10%, no matter the density of the lesion) as long as the lesion diameter exceeds 2 cm. When the lesion diameter drops below 2 cm, significant differences were obtained between MC calculations and the analytic approach (i.e., deviations >10%). As a general rule, the analytic described by Equation (4) tends to overestimate the absorbed dose in small lesions, as the basic assumption of the model is that  $\beta$  radiation is fully absorbed by the tumor or tissue where the decay occurs. When the radius of the tumor is smaller than the maximum range of the  $\beta$  radiation in the medium, a significant amount of the energy is delivered out of the lesion, thus providing smaller absorbed dose values.

Presently, despite the availability of different dose algorithms, the analytic algorithm described by Equation (4) is still widely used to assess the absorbed dose in tumor and in the liver compartment at the clinical level. As a general rule, the size of normal liver is large and Equation (4) provides accurate dose estimates (provided that accurate input parameters are introduced, among which the fractional uptake of the target). However, when this approach is applied to assess the absorbed dose to small tumor masses (i.e., approximately below 2 cm diameter) inaccurate dose estimates can be obtained.

In addition, the analytic algorithm is safely used for treatment planning with glass microspheres. The foundational principle is based on Equation (4), which describes the average dose in a tissue volume as a function of  $^{90}\text{Y}$  activity. During treatment planning, this equation can be solved for the treatment activity  $A_0$ . The results obtained in the present study raise questions as to whether Equation (4) should be used to assess the prescribed  $^{90}\text{Y}$  activity in order to achieve a given tumoricidal endpoint in small liver lesions. This is especially true when intratumoral injection of  $^{90}\text{Y}$  is performed. For example, for HCC 120 Gy should be considered to be a reasonable minimum target dose [21,27,28]. Therefore, when treating an HCC patient with  $^{90}\text{Y}$   $\beta$ -particles, one may wish to set  $D_{tumor}$  to a minimum of 120 Gy. Equation (5) can be rearranged to derive the prescribed treatment activity:  $A(\text{GBq}) = D_{tumor} \cdot m_{tumor}(\text{kg}) / 49.38 \text{ (J/GBq)} \cdot FU_{tumor}$ . Assuming, for example, a tumor mass,  $m_{tumor}$ , of 0.52 g (diameter 1 cm),  $FU_{tumor} = 1$  and  $D_{tumor} = 120 \text{ Gy}$ , Equation (5) would yield a treatment activity of 1.21 MBq (considering  $\rho = 1.05 \text{ g/cm}^3$ ). On the other hand, if Equation (7) is used instead of Equation (4) a prescribed activity of 1.62 MBq is obtained. As previously outlined, the cause of this difference is a result of a significant energy deposition outside the sphere (about 26% of the  $\beta$ -particles energy is delivered outside the sphere, as reported in Figure 1). As a consequence,

a therapeutic activity of 1.21 MBq would actually correspond to an absorbed dose of about 90 Gy, well below the therapeutic endpoint.

As mentioned, the intratumoral injection of  $^{90}\text{Y}$  is likely to pose specific treatment planning issues related to the possibility of treating very small lesions very selectively. In his seminal paper [29], Ariel reported the first interstitial use of  $^{90}\text{Y}$  microspheres for the treatment of a rhabdomyosarcoma. A nodule measuring 1.5 cm in diameter was successfully treated with interstitial injection of 185 MBq of microspheres. In another study [30],  $^{90}\text{Y}$ -glass microspheres were injected into predetermined tumor sites using an ultrasound-guided procedure. Tumor size ranged from 1.9 to 8.8 cm, with most lesions being less than 5 cm in diameter [30]. More recently, Ferrari and co-workers assessed the absorbed doses to small-volumes brain neocavities and surrounding tissues after local  $^{90}\text{Y}$ -DOTATOC injection [5]. A recent review of the literature on the intratumoral treatment with radioactive beta-emitting microparticles can be found in [31].

The evidence from this study suggests that caution must be taken when planning the treatment of very small lesions with  $^{90}\text{Y}$ , implementing the standard analytic approach. This is particularly true when intratumoral administration of  $^{90}\text{Y}$  is performed, as this approach allows sub-centimeters tumors to be selectively treated. In such a scenario, the use of the analytic approach to calculate the therapeutic activity needed to achieve a given tumoricidal endpoint may result in important dose underestimations. On the other hand, Equation (7) can be usefully employed in the treatment planning of spherical lesions of small size (down to 0.5 cm diameter) providing dose estimates in close agreement with Monte Carlo calculations (maximum deviation below 0.5%).

Finally, two potential limitations need to be considered. The first is that in the present study tumor masses were modelled as perfect spheres. The extent to which it is possible to extend the present results to irregular spheres (e.g., oblate spheroids) should be further investigated. Another limitation is that in this study we considered a uniform distribution of the radionuclide into the spheres. As a consequence, the findings might not be representative of situations where the radionuclide is not homogeneously distributed in the tumor region.

## 5. Conclusions

In this paper the absorbed dose in small lesions was assessed using Monte Carlo calculations in a scenario of percutaneous ablation using  $^{90}\text{Y}$  microspheres embedded into a sealant matrix (BAT-90). Furthermore, an analytical formula derived from MC calculations that incorporates the absorbed fractions for  $^{90}\text{Y}$  is proposed. In a scenario of intratumoral injection of microspheres, the proposed equation can be usefully employed in the treatment planning of spherical lesions of small size (down to 0.5 cm diameter) providing dose estimates in close agreement with Monte Carlo calculations (maximum deviation below 0.5%).

**Author Contributions:** Conceptualization, A.A., M.R., M.D., A.S., G.P.; methodology, A.A., M.D., R.C.; simulations, M.D., A.S., L.C.; formal analysis, M.D., A.S., E.M.; investigation, A.A., M.C., G.P.; writing—original draft preparation, M.D., A.A.; writing—review and editing, all authors; visualization, all authors; supervision, A.A.; project administration, A.A., M.R.; funding acquisition, A.A. All authors have read and agreed to the published version of the manuscript.

**Funding:** This research was funded in part by BetaGlue Technologies SpA and the APC was funded by Istituto Scientifico Romagnolo per lo Studio e la Cura dei Tumori (IRST) IRCCS, Meldola, Italy.

**Conflicts of Interest:** A.A. is CEO of BetaGlue Technologies SpA, M.R. is head of operations & quality of BetaGlue Technologies SpA. The other authors declare that they have no competing interests.

## References

1. Villanueva, A. Hepatocellular Carcinoma. *N. Engl. J. Med.* **2019**, *380*, 1450–1462. [[CrossRef](#)] [[PubMed](#)]
2. Hsieh, T.; Wu, Y.; Sun, S.; Yen, K.; Kao, C. Treating Hepatocellular Carcinoma with  $^{90}\text{Y}$ -Bearing Microspheres: A Review. *BioMedicine* **2016**, *6*, 19. [[CrossRef](#)] [[PubMed](#)]

3. Wang, E.; Stein, J.; Bellavia, R.; Broadwell, S. Treatment Options for Unresectable HCC with a Focus on SIRT with Yttrium-90 Resin Microspheres. *Int. J. Clin. Pract.* **2017**, *71*, e12972. [CrossRef] [PubMed]
4. Salem, R.; Hunter, R. Yttrium-90 Microspheres for The Treatment of Hepatocellular Carcinoma: A Review. *Int. J. Radiat. Oncol. Biol. Phys.* **2006**, *66*, S83–S88. [CrossRef] [PubMed]
5. Ferrari, M.; Cremonesi, M.; Bartolomei, M.; Bodei, L.; Chinol, M.; Fiorenza, M.; Tosi, G.; Paganelli, G. Dosimetric model for locoregional treatments of brain tumors with <sup>90</sup>Y-conjugates: Clinical application with <sup>90</sup>Y-DOTATOC. *J. Nucl. Med.* **2006**, *47*, 105–112. [PubMed]
6. Fabbri, C.; Mattone, V.; Casi, M.; De Lauro, F.; Agostini, M.; Bartolini, N.; D’ariento, M.; Marchi, G.; Bartolomei, M.; Sarti, G. Quantitative evaluation on [90Y] DOTATOC PET and SPECT imaging by phantom acquisitions and clinical applications in locoregional and systemic treatments. *Q. J. Nucl. Med. Mol. Imaging* **2012**, *56*, 522–528. [CrossRef] [PubMed]
7. Fabbri, C.; Mattone, V.; Sarti, G.; Casi, M.; De Lauro, F.; Agostini, M.; Bartolini, N.; Bartolomei, M. <sup>90</sup>Y-based PET and SPECT/CT imaging in locoregional brain treatment for high-grade gliomas: Retrospective fusion with MRI. *Eur. J. Nucl. Med. Mol. Imaging* **2012**, *39*, 1822–1823. [PubMed]
8. Beta Glue – A Loco-Regional Radio-Therapy Platform for Tumors. Available online: <https://www.betaglu.com/> (accessed on 1 May 2019). [CrossRef] [PubMed]
9. Arazi, L.; Cooks, T.; Schmidt, M.; Keisari, Y.; Kelson, I. Treatment of solid tumors by interstitial release of recoiling short-lived alpha emitters. *Phys. Med. Biol.* **2007**, *52*, 5025–5042. [CrossRef] [PubMed]
10. Bult, W.; Kroeze, S.; Elschot, M.; Seevinck, P.; Beekman, F.; de Jong, H.; Uges, D.; Kosterink, J.; Luijten, P.; Hennink, W.; et al. Intratumoral Administration of Holmium-166 Acetylacetonate Microspheres: Antitumor Efficacy and Feasibility of Multimodality Imaging in Renal Cancer. *PLoS ONE* **2013**, *8*, e52178.
11. Siegel, J.A.; Stabin, M.G. Absorbed fractions for electrons and beta particles in spheres of various sizes. *J. Nucl. Med.* **1994**, *35*, 152–156.
12. Bardies, M.; Chatal, J. Absorbed doses for internal radiotherapy from 22 beta-emitting radionuclides: Beta dosimetry of small spheres. *Phys. Med. Biol.* **1994**, *39*, 961–981 [CrossRef]
13. Stabin, M.G.; Konijnenberg, M.W. Re-evaluation of absorbed fractions for photons and electrons in spheres of various sizes. *J. Nucl. Med.* **2000**, *41*, 149–160. [CrossRef]
14. Amato, E.; Lizio, D.; Baldari, S. Absorbed fractions for photons in ellipsoidal volumes. *Phys. Med. Biol.* **2009**, *56*, 357–365 [CrossRef]
15. Chao, H.; Torchiana, D. BioGlue: Albumin/Glutaraldehyde Sealant in Cardiac Surgery. *J. Card. Surg.* **2003**, *18*, 500–503
16. Bé, M.-M.; Chisté, V.; Dulieu, C.; Browne, E.; Baglin, C.; Chechev, V.; Kuzmenko, N.; Helmer, R.; Kondev, F.; MacMahon, D.; et al. Table of Radionuclides. Monographie BIPM-5, 2006; 3 Bureau International des Poids et Mesures, Pavillon de Breteuil, F-92310 Sèvres, France. Available online: [http://www.bipm.org/utis/common/pdf/monographieRI/Monographie\\_BIPM-5\\_Tables\\_Vol3.pdf](http://www.bipm.org/utis/common/pdf/monographieRI/Monographie_BIPM-5_Tables_Vol3.pdf) (accessed on 1 May 2019).
17. McKinney, J.; Pasciak, A.; Bradley, Y. *Handbook of Radioembolization*, 1st ed.; CRC Press-Taylor & Francis Group: Boca Raton, FL, USA, 2017.
18. Dezarn, W.; Cessna, J.; DeWerd, L.; Feng, W.; Gates, V.; Halama, J.; Kennedy, A.; Nag, S.; Sarfaraz, M.; Sehgal, V.; et al. Recommendations of the American Association of Physicists in Medicine on dosimetry, imaging, and quality assurance procedures for <sup>90</sup>Y microsphere brachytherapy in the treatment of hepatic malignancies. *Med. Phys.* **2011**, *38*, 4824–4845. [CrossRef]
19. Dieudonné, A.; Hobbs, R.; Sanchez-Garcia, M.; Lebtahi, R. Absorbed-dose calculation for treatment of liver neoplasms with <sup>90</sup>Y-microspheres. *Clin. Transl. Imaging* **2016**, *4*, 273–282. [CrossRef]
20. Ho, S.; Lau, W.; Leung, T.; Chan, M.; Ngar, Y.; Johnson, P.; Li, A. Partition model for estimating radiation doses from yttrium-90 microspheres in treating hepatic tumours. *Eur. J. Nucl. Med.* **1996**, *23*, 947–952. [PubMed]
21. Ho, S.; Lau, W.; Leung, T.; Chan, M.; Johnson, P.; Li, A. Clinical evaluation of the partition model for estimating radiation doses from yttrium-90 microspheres in the treatment of hepatic cancer. *Eur. J. Nucl. Med.* **1997**, *24*, 293–298. [CrossRef] [PubMed]
22. Gulec, S.A.; Mesoloras, G.; Stabin, M. Dosimetric techniques in <sup>90</sup>Y-microsphere therapy of liver cancer: The MIRD equations for dose calculations. *J. Nucl. Med.* **2006**, *47*, 1209–1211. [CrossRef] [PubMed]
23. Briesmeister, J.F. *MCNP-A General Monte Carlo N-Particle Transport Code Version 4C*; Los Alamos National Laboratory: Los Alamos, NM, USA, 2000. [CrossRef]

24. Storm, L.; Israel, H. Photon Cross Sections From 1 Kev To 100 Mev For Elements Z = 1 To Z = 100. *At. Data Nucl. Data Tables* **1970**, *7*, 565–681. [[PubMed](#)]
25. Hubbell, J.; Veigele, W.; Briggs, E.; Brown, R.; Cromer, D.; Howerton, R. Atomic Form Factors, Incoherent Scattering Functions, And Photon Scattering Cross Sections. *J. Phys. Chem. Ref. Data* **1975**, *4*, 471–538. [[CrossRef](#)] [[PubMed](#)]
26. Stabin, M.G.; Sparks, R.B.; Crowe, E. OLINDA/EXM: The second-generation personal computer software for internal dose assessment in nuclear medicine. *J. Nucl. Med.* **2005**, *46*, 1023–1027.
27. Kennedy, A.; Nutting, C.; Coldwell, D.; Gaiser, J.; Drachenberg, C. Pathologic response and microdosimetry of  $^{90}\text{Y}$  microspheres in man: Review of four explanted whole livers. *Int. J. Radiat. Oncol. Biol. Phys.* **2004**, *60*, 1552–1563.
28. Strigari, L.; Sciuto, R.; Rea, S.; Carpanese, L.; Pizzi, G.; Soriani, A.; Iaccarino, G.; Benassi, M.; Ettorre, G.; Maini, C. Efficacy and toxicity related to treatment of hepatocellular carcinoma with  $^{90}\text{Y}$ -SIR spheres: Radiobiologic considerations. *J. Nucl. Med.* **2010**, *51*, 1377–1385.
29. Ariel, I. Cure of an embryonal rhabdomyosarcoma of the nose of an infant by interstitial  $^{90}\text{Y}$  microspheres: A case report. *Int. J. Nucl. Med. Biol.* **1978**, *5*, 37–41.
30. Tian, J.H.; Xu, B.X.; Zhang, J.M.; Dong, B.W.; Liang, P.; Wang, X.D. Ultrasound-guided internal radiotherapy using yttrium-90-glass microspheres for liver malignancies. *J. Nucl. Med.* **1996**, *37*, 958–963.
31. Bakker, R.; Lam, M.; van Nimwegen, S.; Rosenberg, A.; van Es, R.; Nijsen, J. Intratumoral treatment with radioactive beta-emitting microparticles: A systematic review. *J. Radiat. Oncol.* **2017**, *6*, 323–341.



© 2020 by the authors. Licensee MDPI, Basel, Switzerland. This article is an open access article distributed under the terms and conditions of the Creative Commons Attribution (CC BY) license (<http://creativecommons.org/licenses/by/4.0/>).